Bull. Mater. Sci., Vol. 36, No. 7, December 2013, pp. 1153–1160. © Indian Academy of Sciences.

Effect of variation of precursor concentration on structural, microstructural, optical and gas sensing properties of nanocrystalline TiO_2 thin films prepared by spray pyrolysis techniques

LALCHAND A PATIL*, DINESH N SURYAWANSHI, IDRIS G PATHAN and DHANASHRI G PATIL
Department of Physics, Pratap College, Amalner 425 401, India

MS received 12 July 2012; revised 8 September 2012

Abstract. **The objective of the present paper is to investigate the effect of variation of precursor concentration (0·01, 0·02 and 0·03 M) on the structural, microstructural, optical and gas sensing properties of TiO_2 thin films. Titanium dioxide (TiO_2) films were prepared from aqueous solution of titanium chloride ($TiCl_3 \cdot 6H_2O$, 99·9% pure, Merck made, Germany) onto the glass substrates heated at a temperature of 350 °C by the spray pyrolysis technique. Bandgap energy of the films vary from 3·28 to 3·29 eV. X-ray diffraction shows that films to be nanocrystalline with anatase phase having tetragonal crystal structure. The *d* values calculated from electron diffraction patterns (TEM) were observed to be matching with *d* values calculated from XRD. Transmission electron microscopy (TEM) reveled that grain sizes were observed to increase (10–29 nm) with an increase in the concentration of precursor solution. The gas sensing performance of the films was tested.**

Keywords. **Spray pyrolysis; nanocrystalline TiO_2; electron diffraction pattern.**

1. Introduction

Various types of sensors with different operating principles have been explored including the resistive type (Semancik and Cavicchi 1991; Michel *et al* 1998; Dresselhaus and Thomas 2001), thermoelectric (Shin *et al* 2004) and potentiometric (Maffei and Kuriakose 2004). Liquefied petroleum gas (LPG) is a highly inflammable gas. It is explosively utilized in industrial and domestic fields as fuel. It is referred to as town or cooking gas. This gas is potentially hazardous because explosion accidents might be caused, when it leaks out easily. It has been reported that, at concentration up to noticeable leakage, it is very much more than the lower explosive limit (LEL) of the gas in air. There is a great demand and emerging challenges for gas sensors to monitor LPG (Patil *et al* 2006, 2010; Sahay and Nath 2008) for the purpose of control and safe applications in domestic and industrial fields.

Nanostructured materials of nanometer-sized (1–100 nm) particles are particularly interesting for applications in advanced materials that require high reactivity, low superplasticity and unusual electrooptical properties (Panatarani *et al* 2003). In recent years, interest on titanium dioxide have increased tremendously due to its attractive physical, chemical and optical properties (Linsebigier *et al* 1995; Bhuvanesh and Gopal 1997). Nanocrystalline titanium dioxide (TiO_2) offers great attention due to its wide energy gap (3.2 eV), high-electrochemical stability, refractive index and dielectric constant (Diebold 2003More *et al* 2007). TiO_2 is an important semiconductor material, having a wide range of applications such as gas sensors (Hayakawa *et al* 2000; Devi *et al* 2002; Ruiz *et al* 2002, 2004; Zhu *et al* 2002; Chen *et al* 2004), photo-catalysis (Fujishima *et al* 2000; Linkous *et al* 2000; Yang and Davis 2000; Maldoti *et al* 2002; Anpo and Takeuchi 2003), solar cells (Bach *et al* 1998; Grätzel 2001; Adachi 2004). Several methods for the growth of TiO_2 thin films have been reported (Young *et al* 1987; Chaudhari *et al* 2006; Kale *et al* 2006), but they are expensive. On the other hand, chemical spray pyrolysis method is economical and porous structures with high surface area can be grown by a simple method.

Nanostructure TiO_2 thin films were prepared by spray pyrolysis deposition technique (SPD). Because the film formation is carried out in air by a simple apparatus in SPD, technique is one of the most attractive film preparation methods. SPD is essentially pyrosol technique, in which a source solution is sprayed on the heated substrate to be deposited as a film. In other words, when source solutions are atomized, small droplets splash and vapourize on the substrate and leave a dry precipitate in which thermal decomposition occurs (Viguie and Spitz 1975). Organometallic compounds and inorganic salts are used as source materials, which are dissolved in water, ethanol or other solvents to prepare source solutions. Because, the source materials dissolve in a solvent as an ion, oligomer, cluster or sol, depending on their chemical properties. The surface morphology of deposited films are easily controlled by choosing species of the source materials (Okuya *et al* 1999, 2002a, b).

In the present study, we have developed a spray pyrolysis technique to prepare nanocrystalline TiO_2 thin films.

*Author for correspondence (plalachand_phy_aml@yahoo.co.in)

As prepared TiO_2 thin films (0·02 M) give maximum gas response to LPG and H_2 at operating temperatures of 350 and 250 °C, respectively. The effect of precursor concentrations on structural, microstructural, optical and gas sensing properties were studied.

2. Experimental

2.1 *Experimental set up to prepare nanostructured thin films*

Figure 1 shows a chemical spray pyrolysis technique for the preparation of nanocrystalline TiO_2 thin films. Setup consists of spraying chamber, spray gun, air compressor, temperature controller and heater. Transparent, conducting, nanocrystalline TiO_2 thin films were prepared from aqueous solution of $TiCl_3{\cdot}6H_2O$ (99·9% pure, Merck made, Germany) having different concentrations (0·01, 0·02 and 0·03 M). The spray produced by nozzle was sprayed onto the glass substrates heated at 350 °C. Various parameters such as nozzle-to-substrate distance, deposition time, flow rate of solution and deposition temperature were optimized to obtain films of good quality.

2.2 *Preparation of nanocrystalline TiO_2 thin films*

For the deposition of TiO_2 thin films by spray pyrolysis, the precursor solution was prepared by dissolving titanium chloride ($TiCl_3{\cdot}6H_2O$, 99·9% pure, Merck made, Germany) in double-distilled water. The spraying solution concentrations were: 0·01, 0·02 and 0·03 M. Table 1 shows preparative conditions of nanocrystalline TiO_2 thin films using spray pyrolysis.

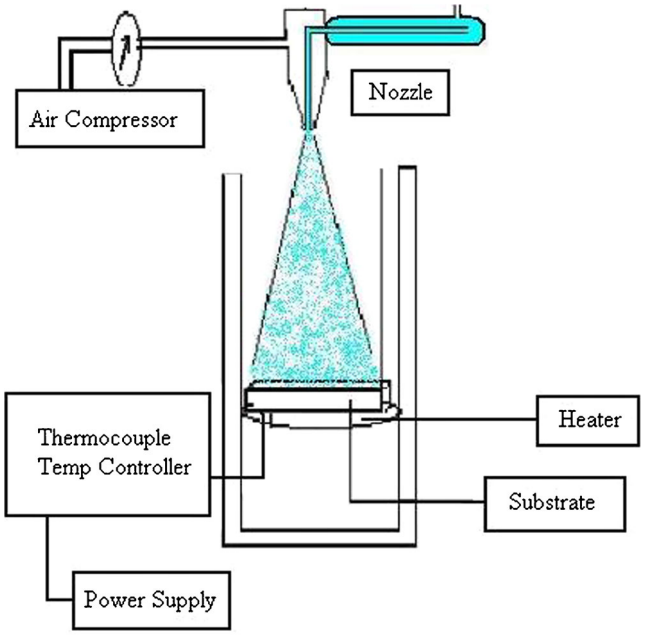

Figure 1. Spray pyrolysis system set up.

2.3 *Details of gas sensing system*

The sensing performance of the sensors was examined using "static gas sensing system" explained elsewhere (Jain *et al* 2006).

3. Characterization of nanocrystalline TiO_2 thin film and results

The structural analysis of nanocrystalline TiO_2 thin films was carried out by XRD (Rigaku DMAX 2500) with CuKα radiation at a wavelength of 1·5418 Å. Electron diffraction patterns of nanocrystalline TiO_2 thin films were obtained using TEM (Philips EM 400). A UV–Visible spectrophotometer (Shimadzu 2450 UV–Vis) was used to study the optical properties of nanocrystalline TiO_2 thin films. The thickness and roughness of thin films were measured by using Surface Profiler [AMBIOS Tech. (USA) XP-I].

3.1 *Thickness and roughness determination of TiO_2 thin films*

The thickness of thin films was measured (table 2) by using Surface Profiler (AMBIOS Tech. (USA) XP.I) having a vertical resolution of 1·5 Å, lateral resolution of 100 nm and lateral length of 200 nm. It is clear from table 2, that thicknesses of nanocrystalline TiO_2 sample are increasing with increase in precursor concentration. Roughness of sample *S*2 is higher than the roughness of samples *S*1 and *S*3.

3.2 *Structural properties: X-ray diffraction studies*

Figure 2 shows XRD spectra of samples *S*1, *S*2 and *S*3. The observed "*d*" values of TiO_2 confirmed that the deposited films are of TiO_2 anatase phase with tetragonal structure matching well with ASTM data book, card no. 21-1272. One additional minor peak along (213) is observed for thicker film (*S*3). In XRD pattern, (101) peak has the most distinct reflection. So, the mean crystalline size is calculated with the line broadening of (101) reflection (*S*1, *S*2 and *S*3) using well known Scherrer equation (1):

$$d = 0{\cdot}9\lambda/\beta\cos\theta \qquad (1)$$

where d is crystallite size, β the full width at half maxima in radian and λ is the wavelength of X-ray (1·5418 Å). The crystallite size was observed to be increasing with precursor concentration as presented in table 3.

Crystallinity of the material has direct dependence on the film thickness. Crystallinity has been observed to improve with an increase of the film thickness (Chang *et al* 2002). Moreover, the increase of crystallite size could be attributed to the improvement of crystallinity and an increase in the cluster formation leading to agglomeration of small crystallites. These agglomerated crystallites coalesce together

Table 1. Process parameters for spray deposition of TiO_2 thin films.

Sample	Concentration (M)	Pyrolysis temp. (°C)	Firing temp. (°C)	Compressed air (kg/cm^2)	Spray rate (ml/min)
*S*1	0·01	350	550	2·5	4·9
*S*2	0·02	350	550	2·5	4·9
*S*3	0·02	350	550	2·5	4·9

resulting in the formation of larger crystallites with better crystallinity.

3.3 *Microstructure and electron diffraction using TEM*

Figures 3(a), (c) and (e) show transmission electron micrograph [CM 200 Philips (200 kV HT)] of powders obtained by scratching the thin film samples: *S*1, *S*2 and *S*3 respectively. The powder was dispersed in ethanol. TEM uses copper grid to hold the powder. The sample particles on the grid were scanned in all the zones before the picture was taken. Figure 3(a) shows that grains are spherical or ellipsoidal in nature with an average grain size of 10 nm. It is clear from figure 3(c) that large number of grains are distributed randomly having spindle shape with an average grain size of 22 nm. Figure 3(e) shows that grains distributed randomly having spindle shape with an average grain size of 29 nm. It is clear from table 4 that the grain size of samples (*S*1, *S*2 and *S*3) is increasing with increase in precursor concentration.

Figures 3(b) and (d) show electron diffraction patterns of *S*1 and *S*2 samples, respectively. The electron diffraction patterns show clear and continuous ring patterns revealing their polycrystalline structure. Five fringe patterns corresponding to planes: (1 0 1), (0 0 4), (2 0 0), (2 1 1) and (2 0 4) are consistent with the peaks observed in XRD patterns. XRD and TEM studies confirmed pure tetragonal structure of TiO_2 as evidenced from figures 2 and 3, respectively.

The distance from centre to each ring (moving from the smallest to larger ones) is measured to be 2·801, 4·211, 5·402, 6·121 and 6·970 nm, respectively for samples *S*1 and 2·790, 4·271, 5·462, 6·170 and 7·100 nm, respectively for sample *S*2. This is indicated in figures 3(b) and (d) and expressed in terms of nm^{-1}. The reciprocal of these values give the interplanar distance *d*. Details are given in table 5.

It is clear from table 5 that *d* values calculated from electron diffraction patterns (TEM) of nanocrystalline TiO_2 thin films matched with *d* values calculated from XRD.

Table 2. Thickness and roughness of TiO_2 thin films for different concentrations.

Sample	Concentration (M)	Thickness (nm)	Roughness (nm)
*S*1	0·01	223·8	33·3
*S*2	0·02	534·2	82·7
*S*3	0·03	652·2	33·9

3.4 *Optical absorption*

Figure 4 shows variation of absorbance with wavelength of nanocrystalline TiO_2 thin films in the range of 300–600 nm. The bandgap energy of the samples was calculated from the absorption edges of the spectra (Bari *et al* 2006). The bandgap was observed to be slightly varying from 3·28 to 3·29 eV. Bandgap of *S*1 < *S*2, bandgap of *S*2 < bandgap of *S*3. These values nearly match with the reported value of TiO_2, i.e. 3·2 eV (Brady 1971; Daude *et al* 1977; Tang *et al* 1994). It is clear from the absorption spectra that concentration does not affect much for the bandgap energy of nanocrystalline TiO_2 thin films.

4. Electrical properties of sensor

4.1 *I–V characteristics*

Figure 5 shows *I–V* characteristics of nanostructured TiO_2 thin films. The graphs are observed to be symmetrical in nature indicating ohmic contact.

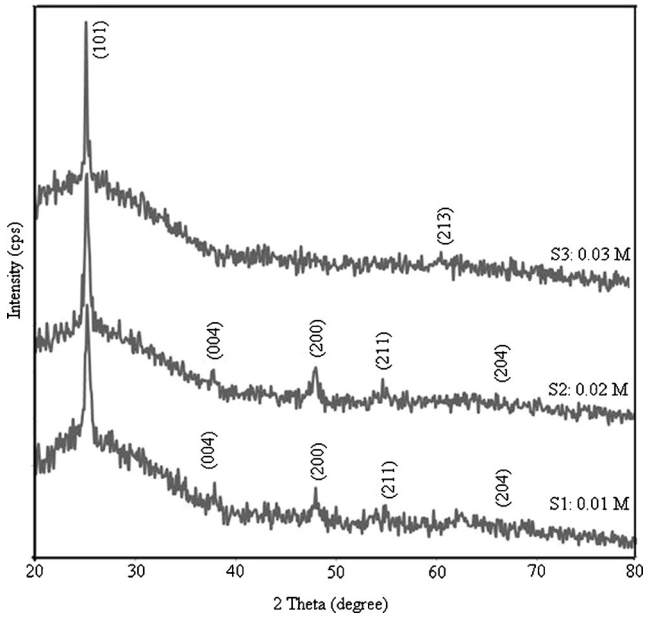

Figure 2. X-ray diffraction spectra of samples: *S*1 (0.01 M), *S*2 (0.02 M) and *S*3 (0.03 M).

5. Sensing performance of the sensor

5.1 *Gas sensing performance of thin film resistors*

The thin film sensors mounted on static gas sensing system (Jain *et al* 2006; Wagh *et al* 2006; Patil *et al* 2007) were tested on exposure of ethanol, carbon dioxide, LPG, ammonia, chlorine and hydrogen. Values of current before and after exposure of gas were measured and gas responses at various operating temperatures were determined.

Table 3. Grain size calculated from XRD.

Sample	Concentration (M)	Grain size calculated from XRD (nm)
*S*1	0·01	9·24
*S*2	0·02	21·70
*S*3	0·03	29·50

5.2 *Measurement of gas response and selectivity*

Gas response (S) is defined as the ratio of the change in conductance of the sensor on exposure to the target gas to the original conductance in air. The relation for S is given as

$$S = (G_g - G_a)/G_a, \tag{2}$$

where G_a and G_g are the conductance of sensor in air and in a target gas medium, respectively.

Selectivity or specificity is defined as the ability of a sensor to respond to a certain gas in the presence of other gases.

5.3 *Variation of gas response with operating temperature for LPG and H_2*

Figures 6(a) and (b) show variation of LPG and H_2 responses with operating temperature, respectively. It is clear from

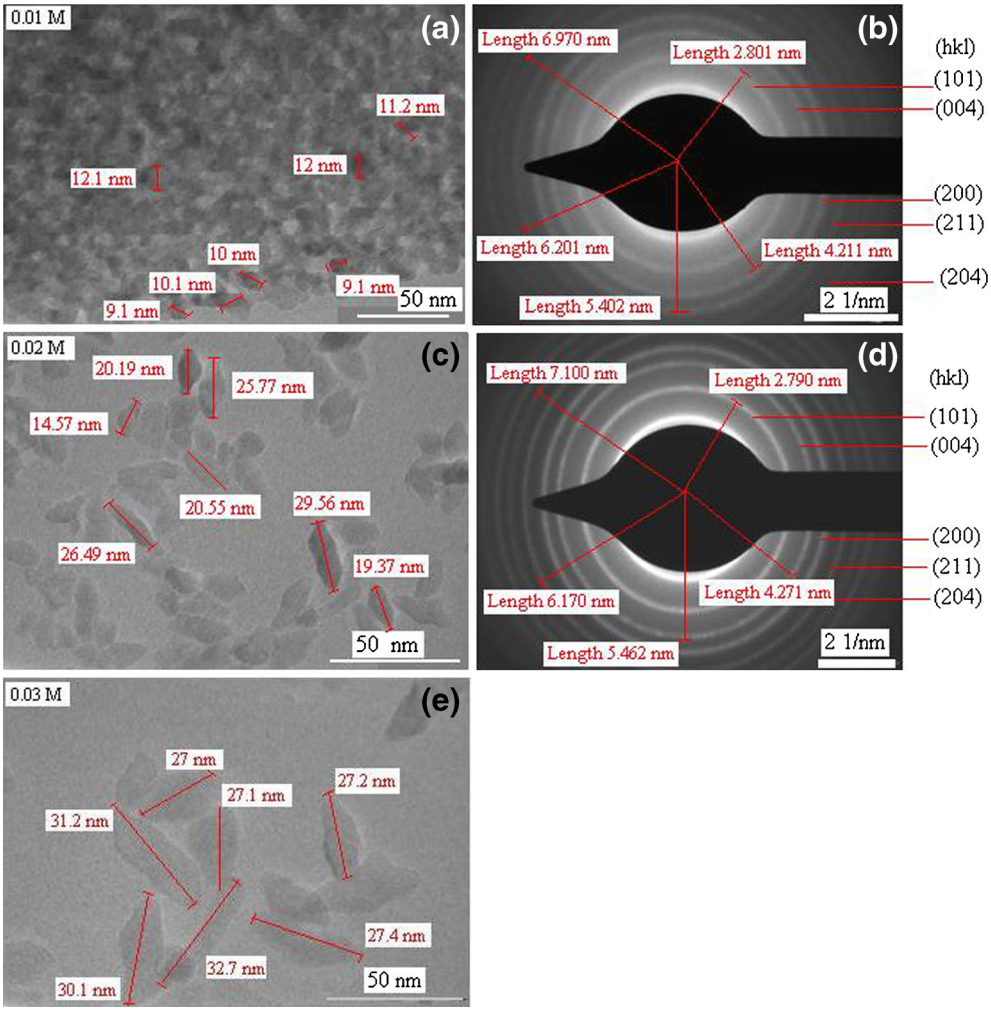

Figure 3. (**a**) TEM image, (**b**) electron diffraction image of sample *S*1, (**c**) TEM image, (**d**) electron diffraction image of sample *S*2 and (**e**) TEM image of sample *S*3.

figures 6(a) and (b) that gas response of each sample increases with operating temperature, reaches to a maximum for LPG ($S = 82$) at 350 °C, for H_2 ($S = 54$) at 250 °C (sample *S*2) and falls with further increase in operating temperature. Sensor *S*2 is most sensitive to LPG at 350 °C and to H_2 at 250 °C as compared to sensors *S*1 and *S*3.

It is clear from table 2 that roughness of sample *S*2 is more as compared to samples *S*1 and *S*3. Surface roughness of films are important because it affects shift in electronic energy levels and degrades electrical characteristics (Young-Bae *et al* 2003). Porosity of thin film is related to the surface roughness. Roughness of sample *S*2 is higher than *S*1 and *S*3. This may be the reason that sample *S*2 gives the highest gas response to LPG and H_2 as compared to *S*1 and *S*3.

High sensitivity of *S*2 may be due to optimum particle size which would have created good porosity and hence, high effective surface area in the film. Higher the surface area for interaction with exposed gas, higher would be the sensitivity to the gas. Smaller particles in case of film *S*1 may not allow the film to be too porous. This hampers the effective area. Larger particle in case of *S*3 may not result into high effective surface area to interact with the gas.

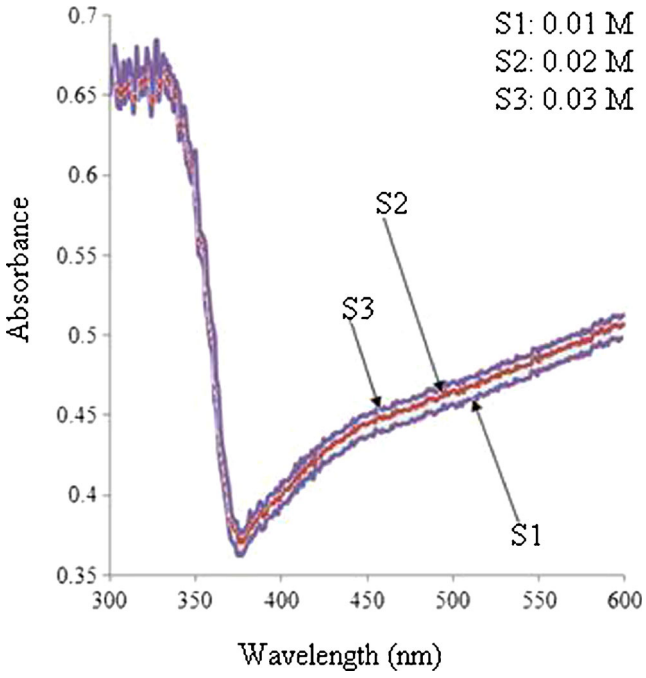

Figure 4. Absorption spectra of samples *S*1, *S*2 and *S*3.

5.4 *Selectivity of LPG and H_2 against various gases*

Figure 7(a) shows selectivity of *S*1, *S*2 and *S*3 thin films to LPG against H_2, CO_2, $NH_3{\cdot}Cl_2$ and ethanol gases at 350 °C. Figure 7(b) shows selectivity to H_2 against LPG, CO_2, $NH_3{\cdot}Cl_2$ and ethanol gases at 250 °C. It is clear from the figure that nanostructured TiO_2 thin films *S*1, *S*2 and *S*3 were found to be highly selective to LPG and H_2 at 350 and 250 °C, respectively against other gases. The most important reason of this outstanding performance is the nanocrystalline nature of TiO_2 film.

Table 4. Grain size observed from TEM.

Sample	Concentration (M)	Grain size observed from TEM (nm)
*S*1	0·01	10
*S*2	0·02	22
*S*3	0·03	29

5.5 *Reproducible sensing cycles of TiO_2 thin films (S1, S2 and S3)*

Reproducible behaviour of each sample was tested by conducting 10 similar cycles of gas sensing process. The sensitivity values of each sample was observed to be approximately similar as shown in figures 8(a) and (b).

6. Discussion

TiO_2 based thin film (*S*1, *S*2 and *S*3) samples were exposed with six types of gases: LPG, H_2, CO_2, $NH_3{\cdot}Cl_2$ and ethanol.

Table 5. *d* values obtained from XRD and TEM.

	X-ray diffraction (XRD) *d* values		Electron diffraction (TEM) Sample *S*1		Electron diffraction (TEM) Sample *S*2		
Reported *d* values	Sample *S*1	Sample *S*2	Reciprocal of *d* values δ_{hkl} (nm^{-1})	*d* values δ_{hkl} (nm)	Reciprocal of *d* values δ_{hkl} (nm^{-1})	*d* values δ_{hkl} (nm)	Planes (*hkl*)
3·5200	3·5107	3·5107	2·801	3·5714	2·790	3·5842	101
2·3780	2·3812	2·3812	4·211	2·3752	4·271	2·3419	004
1·8920	1·8911	1·8911	5·402	1·8518	5·462	1·8313	200
1·6665	1·6411	1·6411	6·121	1·6339	6·170	1·6207	211
1·4808	1·4712	1·4712	6·970	1·4317	7·100	1·4084	204

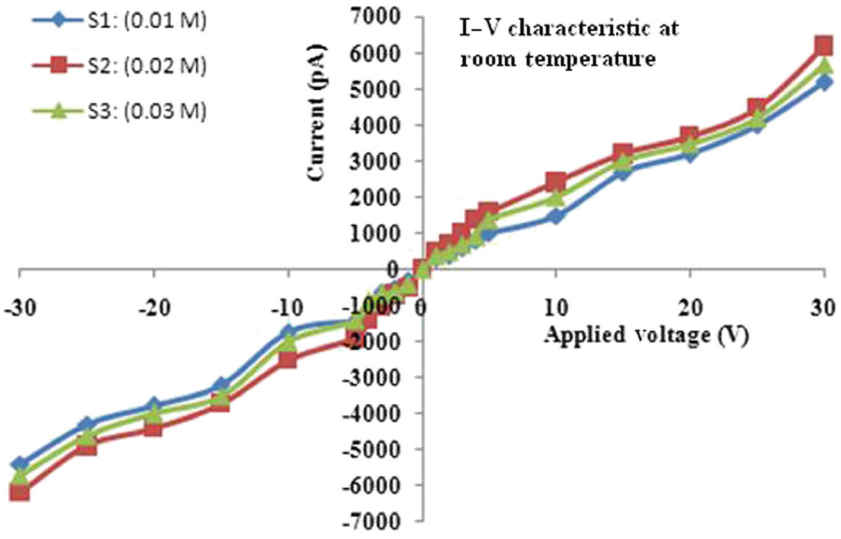

Figure 5. *I–V* characteristics of TiO_2 thin films.

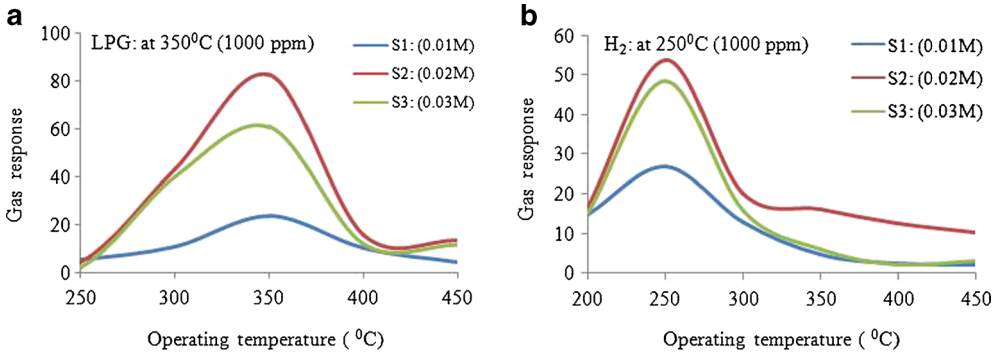

Figure 6. Variation of gas response with operating temperature for (**a**) LPG and (**b**) H_2.

It was responding more or less to all the gases. The samples showed temperature dependent sensing, i.e., the same sample responded to two gases at two different operating temperatures. The same sample may be used to detect two gases just by tuning the respective operating temperature corresponding to the gas. LPG sensitivity values of *S*2 and *S*3 at 350 °C were 82 and 61, respectively which were observed to be larger than their sensitivity values (54 and 48, respectively) to H_2 at 250 °C. Selectivity values of LPG and H_2 are relatively larger against CO_2, $NH_3{\cdot}Cl_2$ and ethanol.

6.1 *LPG sensing*

Response of sensors depends on two factors, viz. the speed of chemical reaction on the surface of the grains and speed of diffusion of gas molecules to that surface. At low temperatures, the sensor response is restricted by the speed of chemical reactions. At higher temperature, the sensor response is restricted by the speed of the diffusion of gas molecules to that surface. At some intermediate temperature, the speed values of two processes become equal and at that point the sensor response reaches its maximum. According to this mechanism, for every gas there is a specific temperature at which the sensor response attains its peak value.

When TiO_2 thin film is exposed to LPG, the hydrocarbons viz. propane (C_3H_8) and butane (C_4H_{10}) present in LPG interact with the adsorbed oxygen ions present on the surface of the sensor. The hydrocarbons are converted to CO_2 and H_2O due to their interaction with the adsorbed oxygen ions. The overall reaction of LPG molecules with adsorbed oxygen species can be explained based on the following reactions (Sahay and Nath 2008):

$$O_{2(nds)} + e^- \rightarrow O^-_{2\,(ads)}, \tag{3}$$

$$O^-_{2(ads)} + e^- \rightarrow 2O^-_{(ads)}, \tag{4}$$

$$C_nH_{2n+2} + 2O^-_{(ads)} \rightarrow H_2O + C_nH_{2n} : O + e^-, \tag{5}$$

$$C_nH_{2n} : O + O^-_{(ads)} \rightarrow CO_2 + H_2O + e^-, \tag{6}$$

where C_nH_{2n+2} denote C_3H_8, C_4H_{10}, etc and C_nH_{2n}:O represents partially oxidized intermediates on TiO_2 surface. This

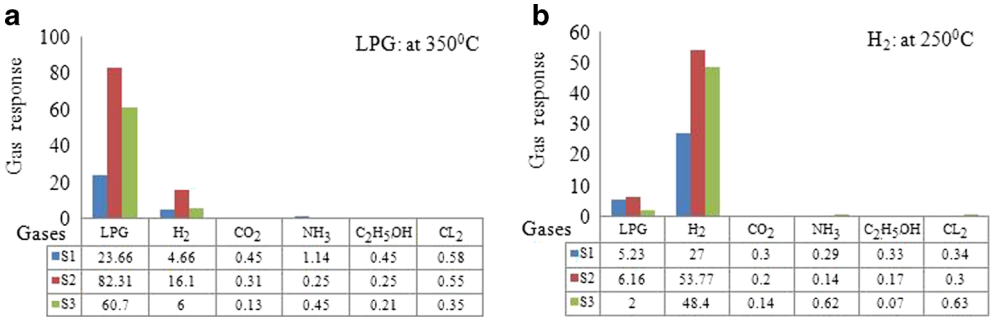

Gases	LPG	H_2	CO_2	NH_3	C_2H_5OH	CL_2
S1	23.66	4.66	0.45	1.14	0.45	0.58
S2	82.31	16.1	0.31	0.25	0.25	0.55
S3	60.7	6	0.13	0.45	0.21	0.35

Gases	LPG	H_2	CO_2	NH_3	C_2H_5OH	CL_2
S1	5.23	27	0.3	0.29	0.33	0.34
S2	6.16	53.77	0.2	0.14	0.17	0.3
S3	2	48.4	0.14	0.62	0.07	0.63

Figure 7. Selectivity of sample *S*2: (**a**) LPG at 350 °C and (**b**) H_2 at 250 °C against various gases.

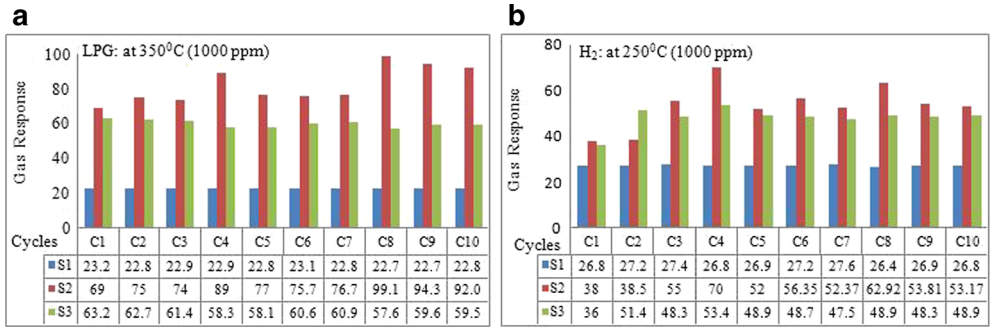

Cycles	C1	C2	C3	C4	C5	C6	C7	C8	C9	C10
S1	23.2	22.8	22.9	22.9	22.8	23.1	22.8	22.7	22.7	22.8
S2	69	75	74	89	77	75.7	76.7	99.1	94.3	92.0
S3	63.2	62.7	61.4	58.3	58.1	60.6	60.9	57.6	59.6	59.5

Cycles	C1	C2	C3	C4	C5	C6	C7	C8	C9	C10
S1	26.8	27.2	27.4	26.8	26.9	27.2	27.6	26.4	26.9	26.8
S2	38	38.5	55	70	52	56.35	52.37	62.92	53.81	53.17
S3	36	51.4	48.3	53.4	48.9	48.7	47.5	48.9	48.3	48.9

Figure 8. Repetition of gas response for samples *S*1, *S*2 and *S*3: (**a**) LPG at 350 °C and (**b**) H_2 at 250 °C.

reaction produces CO_2 and H_2O and releases the trapped electrons back to the conduction band of TiO_2. As a result the resistance of TiO_2 thin films decreases and conductivity increases upon exposure to LPG.

6.2 *H_2 sensing*

It is well known that oxygen molecules are adsorbed on the surface of TiO_2 to form O_2, O and O^2 ions by abstracting electrons from the conduction band of TiO_2 depending on temperature. The oxygen species are O_2 molecules below 100 °C, O_2^- between 100 and 300 °C, and O^{2-} above 300 °C (Choi *et al* 2009).

$$H_{2(ads)} + O^-_{(ads)} \rightarrow H_2O_{(gas)} + e^-. \quad (7)$$

When TiO_2 thin films are exposed to H_2 gas, H_2 gas reacts with the adsorbed O^- ions on the surface of TiO_2 thin films according to (7). Then electrons are returned back to the films. Increase of electrons decreases the resistance of TiO_2 thin films and conductivity increases upon exposure to H_2.

7. Conclusions

Simple spray pyrolysis technique was observed to be useful for the preparation of nanostructure films of TiO_2. The size of TiO_2 nanoparticles varies with variation in the concentration of precursor solution. The grain sizes (*S*1, *S*2 and *S*3) calculated from XRD match well with the grain sizes (*S*1, *S*2 and *S*3) observed from TEM. The *d* values (*S*1 and *S*2) calculated from XRD and *d* values (*S*1 and *S*2) calculated from electron diffraction patterns (TEM) are similar. Nanocrystalline TiO_2 thin films were observed to be sensitive to LPG at 350 °C and to hydrogen at 250 °C. The films may be useful for the fabrication of temperature dependent sensor. Nanocrystalline nature was observed to be useful in gas sensing. TiO_2 films showed repeatable gas sensing performance.

Acknowledgements

The authors are thankful to Head of the Department of Physics and Principal, Pratap College, Amalner, for providing laboratory facilities for this work. Authors are also thankful to Principal, Prof BV Patil, Rani Laxmibai College, Parola.

References

Adachi M 2004 *J. Am. Chem. Soc.* **126** 14943
Anpo M and Takeuchi M 2003 *J. Catal.* **216** 505
Bach U, Lupo D, Comte P, Moser J A, Weissortel F, Salbeck J, Spreitzer H and Grätzel M 1998 *Nature* **395** 583
Bari R H, Patil L A and Patil P P 2006 *Bull. Mater. Sci.* **29** 529
Bhuvanesh N S P and Gopal K J 1997 *J. Mater. Chem.* **7** 297
Brady G S 1971 *Materials handbook* (New York: McGraw-Hill)
Buechler K J, Noble R D, Koval C A and Jacoby W A 1999 *Ind. Eng. Chem. Res.* **38** 892

Chaudhari G N, Bambole D R, Bodade A B and Padole P R 2006 *J. Mater. Sci.* **41** 4860
Chang J F, Kuo H H, Leu I C and Hon M H 2002 *Sens. Actuators* **B84** 258
Chen W, Fang Q, Li S, Wu J, Li F and Jiang K 2004 *Sens. Actuators* **B100** 195
Daude N, Gout C and Jouanin C 1977 *Phys. Rev.* **B15** 3229
Devi G S, Hyodo T, Shimizu Y and Egashira M 2002 *Sens. Actuators* **B87** 122
Diebold U 2003 *Surf. Sci. Rep.* **48** 53
Dresselhaus M S and Thomas I L 2001 *Nature* **414** 332
Fujishima A, Rao T N and Tryk D A 2000 *J. Photochem. Photobiol. Photochem. Rev.* **1** 1
Grätzel M 2001 *Nature* **414** 338
Hayakawa I, Wamoto I Y, Kikuta K and Hirano S 2000 *Sens. Actuators* **B62** 55
Jain G H, Patil L A, Wagh M S, Patil D R, Patil S A and Amalnerkar D P 2006 *Sens. Actuators* **B117** 159
Kale S S, Mane R S, Chung H, Yoon M Y, Lokhande C D and Han S H 2006 *Appl. Surf. Sci.* **253** 421
Linsebigier A L, Lu G and Yates T 1995 *Chem. Rev.* **3** 775
Linkous C A, Carter G J, Locuson D B, Ouellette A J, Slattery D K and Smitha L A 2000 *Environ. Sci. Technol.* **344** 754
Maffei N and Kuriakose A K 2004 *Sens. Actuators* **B98** 73
Maldoti A, Molinari A and Amadeni R 2002 *Chem. Rev.* **102** 3811
Michel H J, Leiste H, Schierbaum K D and Halbritter J 1998 *Appl. Surf. Sci.* **126** 57
More A M, Gunjkar J L, Lokhand C D, Man R S and Han S H 2007 *Micron.* **38** 500
Okuya M, Prokudina N A, Mushika K and Kaneko S 1999 *J. Eur. Ceram. Soc.* **19** 903
Okuya M, Kaneko S, Prokudina N A, Fujiwara T and Murakami K 2000 *Ceram. Trans.* **109** 473
Okuya M, Nakade K and Kaneko S 2002a *Sol. Energy Mater. Sol. Cells* **70** 473
Okuya M, Osa D and Kaneko S 2002b *Key Eng. Mater.* **247** 228
Okuya M, Nakade K, Osa D, Nakano T, Kumara G R A and Kaneko S 2004 *J. Photochem. Photobiol. A Chem.* **164** 167
Oh and Choi E et al 2009 *Sens. Actuators* **B141** 239
Patil D R, Patil L A, Jain G H, Wagh M S and Patil S A 2006 *Sens. Trans.* **74** 883
Patil L A, Bari A R, Shinde M D and Deo Vinita 2010 *Sens. Actuators* **B149** 79
Patil S A, Patil L A, Patil D R, Jain G H and Wagh M S 2007 *Sens. Actuators* **B123** 233
Panatarani C I, Lenggoro W and Okuyama K J 2003 *Nanopart. Res.* **5** 47
Ruiz A M, Cornet A and Morante J R 2004 *Sens. Actuators* **B100** 256
Sahay P P and Nath R K 2008 *Sens. Actuators* **B133** 222
Ruiz A, Arbiol J, Cirera A, Cornet A and Morante J R 2002 *Mater. Sci. Eng.* **C19** 105
Semancik S and Cavicchi R E 1991 *Thin Solid Films* **206** 81
Shin W, Matsumiya M, Qiu F, Izu N and Murayama N 2004 *Sens. Actuators* **B97** 344
Tang H, Prasad K, Sanjines R, Schmid P E and Levy F 1994 *J. Appl. Phys.* **75** 2042
Viguie J C and Spitz J 1975 *J. Electrochem. Soc.* **122** 583
Wagh M. S, Jain G H, Patil D R, Patil S A and Patil L A 2006 *Sens. Actuators* **B115** 128
Yang J K and Davis A P 2000 *Environ. Sci. Technol.* **343** 796
Young V Y, Chang F C and Cheng K L 1987 *Appl. Spectrosc.* **41** 994
Young-Bae P, Ahn K H and Dong-Wha P 2003 *J. Mater. Sci. Lett.* **V22** 1325
Zhu Y, Shi J, Zhang Z, Zhang C and Zhang X 2002 *Anal. Chem.* **74** 120